Available online at www.sciencedirect.com

SciVerse ScienceDirect

Ceramics International 39 (2013) 709–718

CERAMICS INTERNATIONAL

www.elsevier.com/locate/ceramint

Uncovering the critical factor in determining the residual stresses level in Si_3N_4–GM filler alloy–42CrMo joints by FEM analysis and experiments

Yanming He[a,b], Jie Zhang[a,*], Feng Pan[a], Chunfeng Liu[a], Xiaodong Li[b,*]

[a]School of Materials Science and Engineering, Harbin Institute of Technology, Harbin 150001, China
[b]Department of Mechanical Engineering, University of South Carolina, 300 Main Street, Columbia, SC 29208, USA

Received 5 April 2012; received in revised form 24 June 2012; accepted 25 June 2012
Available online 3 July 2012

Abstract

The influence of gradient materials (GM) filler alloy on the distribution of thermal stresses and on the bending strength of the brazed Si_3N_4–42CrMo steel joints was examined by using finite element modeling (FEM) computations in combination with experiments. In order to form a smooth thermal expansivity change across the whole joint, a novel GM filler alloy was fabricated by stacking each layer with different content of Mo particles (Ag–Cu–Ti+Mo) addition together. We examined the effect of GM compositions, layer numbers and thicknesses on the residual stresses in the brazed joint. In particular, the monolayer composite filler produced by incorporating 10 vol% Mo particles induced the minimum residual stresses in the joint, agreeing with the experimental results. The results indicated that the CTE mismatch between the joined materials and the ability of plastic deformation in the filler alloy were two factors that determine the residual stresses level in a brazed joint. The results reported here will provide us guidance to choose an appropriate filler alloy for improving the ceramic–metal joint performance.

Keywords: A. Joining; C. Mechanical properties; D. Si_3N_4; Finite element method

1. Introduction

Silicon nitrides possess excellent mechanical properties and good corrosion resistance at room or high temperatures, which makes them ideal for advanced structural applications. Nevertheless, in order to meet strict application requirements, the reliable joining techniques become crucial [1]. For applications in such conditions, the active filler metals, such as Ag–Cu–Ti, have been commonly employed in joining Si_3N_4 to themselves or to metallic parts [2]. The residual stresses are usually generated near the bonding interface when cooling from the bonding temperature due to the discontinuity in thermal and elastic properties of the joined materials [3–5]. Most metals are softer than ceramics and have larger thermal expansion coefficients (CTE). The thermal residual stress can aggravate the mechanical properties of the ceramic–metal joints, and may cause catastrophic fracture [6]. Lots of researches believed that the stress level in these joints can strongly be dependent on the thermal expansion and elastic modulus mismatches between the joined materials. Nevertheless, our research group [7] indicated that the ability of plastic deformation in the filler alloy also played an important role. A key question, therefore, should be addressed: which is the main factor that determines the residual stress level in a brazed joint? An investigation of the distribution and magnitude of the residual stress in the joint should be carried out in order to answer above questions. For calculating the residual stress in a brazed joint, a finite element method (FEM) is effective since it can determine precisely the stress distribution across the whole joint if the precise data for the joined materials are supplied [8].

Another critical problem is how to decrease the CTE mismatches in the ceramic–metal configuration.

*Corresponding authors.
E-mail addresses: hitzhangjie@hit.edu.cn (J. Zhang), lixiao@cec.sc.edu (X. Li).

0272-8842/$36.00 © 2012 Elsevier Ltd and Techna Group S.r.l. All rights reserved.
http://dx.doi.org/10.1016/j.ceramint.2012.06.082

The interlayers were usually introduced in the filler alloy, such as soft metal interlayers, laminate interlayers and fine crack interlayers [9,10]. Besides, incorporation of ceramic particles or fiber reinforcements into the filler alloy was proved to be effective [11–14]. We have reported the addition of 10 vol% Mo particles to 66.24Ag–25.76Cu–8Ti (wt%) filler alloy for the joining Si_3N_4 ceramic and 42CrMo steel, and a high joint strength was obtained [15]. The concept of graded material (GM) was initially proposed in Japan and introduced into the joining of ceramics ten years ago [16], which was considered to be a novel and effective way to accommodate the residual stresses theoretically. The GM filler alloy can produce a gradual composition change from one joining substrate to another, with a gradual CTE change, thereby avoiding the abrupt changes in the mechanical properties across the bonding interface. However, most of GM interlayers that were introduced in the past were essentially comprised of two joined parent materials [17–20]. This paper presents, for the first time as we know, Ag–Cu–Ti filler alloy with different Mo particles addition and stack each layer together to form the GM filler alloy. The FEM analysis were used to compute the magnitude and distribution of the residual stresses in the joint, supplying an explicit understanding of stresses state in the joint and thereby guiding us to design the GM filler alloy. On that basis, the critical factor that determines the residual stresses level in a brazed joint was uncovered. In addition to this, the elaborate GM was also introduced into joining the Si_3N_4 ceramic to 42CrMo steel.

2. Experiments

2.1. Materials

The Si_3N_4 ceramic and 42CrMo steel were tailored into the required dimensions (3 mm × 4 mm × 17 mm). The brazing surface (3 mm × 4 mm) of the ceramic and steel was prepared by standard polishing. The filler alloy was composed of 69.12Ag–26.88Cu–4Ti (wt%) alloy powder with an average particle size of 50 μm, and Mo particles with an average diameter of 10 μm. The mechanical alloying method was introduced into preparing the monolayer composite filler with different content of Mo particles addition. The details on the preparation of composite filler were discussed in previous work [15]. The GM filler alloy with gradual composition was produced by stacking each layer with different percentage of Mo particles addition together. In order to create a gradual CTE change from the Si_3N_4 ceramic to 42CrMo steel, the Mo-rich composite layer should be placed close to the Si_3N_4 ceramic, while the composite layer with the lower content of Mo particles was put near the 42CrMo steel. Before stacking, the binder was added in each layer and the composite paste was dried with a blower. The assembly was brazed at 900 °C, soaked for 10 min. The brazed joints were observed using SEM and EDS on a FEI Quanta 200F electron microscope. The strength of the butt joint was measured by three-point bending test with a cross-head speed of 0.5 mm/min. At least three samples were used to determine the bending strength of the joint for each joining condition.

2.2. Model description

The continuum models were used to compute the strains and stresses in the joint. The stress-free temperature was set at 780 °C, which is the melting point of Ag–Cu filler alloy. A spatially uniform cooling was assumed during computation. The gradual filler alloy was treated as a series of perfectly bonded composite interlayers and each layer was assigned with different properties, i.e. CTE, elastic modulus, and yield stress. Numerical solutions were carried out with the Ansys10.0 computer program. The eight-node quadrilaterial Solid 45 element that includes mechanical and thermal capacities was chosen. A tridimensional thermal elasto–plastic model was generated, as schematically indicated in Fig. 1(a), whose dimension was equal to the actual size of the studied specimens, i.e. 3 mm × 4 mm × 34 mm. The interfacial reaction layer at the Si_3N_4 ceramic/filler alloy interface was considered during computation. The mesh was refined near the bonding interface where the larger residual stresses were expected, as shown in Fig. 1(b). In order to create an actual simulation environment, one of the corners in the

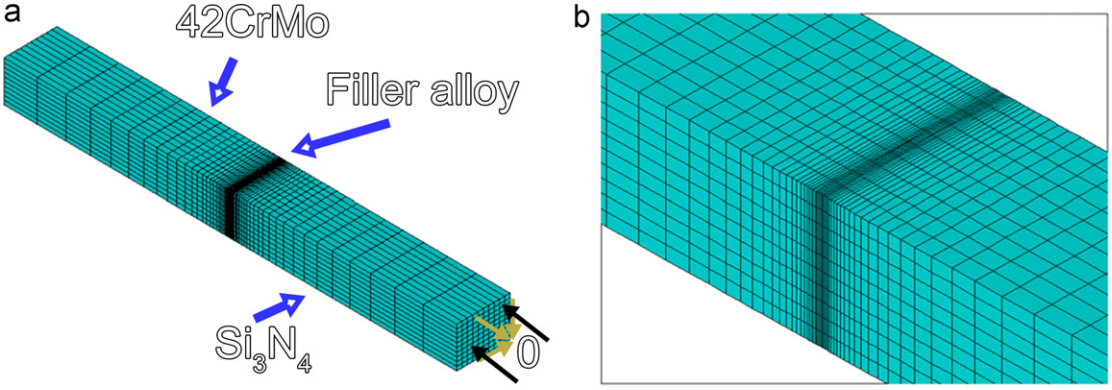

Fig. 1. Typical finite element mesh in FEM calculation: (a) entire mesh; (b) the mesh refinement near the interface.

Table 1
Basic materials properties used in the computations.

Materials	Temperature (°C)	Elastic modulus (GPa)	CTE ($\times 10^{-6}$ °C^{-1})	Yield stress (MPa)	Poisson's ratio
Si_3N_4	–	320	3.28	> 700	0.25
TiN	–	350	9.35	–	0.22
Mo	–	320	5.7	450–550	0.29
Ag–Cu–Ti	20	93.6	19.0	230	0.35
	100		19.5	202	
	200	85	19.7	170	
	300		19.9	135	
	400	79.4	20.2	98	
	500		20.3	60	
	600	70.2	20.5	25	
	700		20.5		
	800	58.1	21	20	0.28
42CrMo	20	210		805	
	100		11.1	720	
	200		12.1	695	
	300	185	12.9	625	
	400	175	13.5	550	
	500	165	13.9		
	600	155	14.1		

Si_3N_4 ceramic was fixed in three directions, and its bottom was also fixed in axial direction, as indicated in Fig. 1(a).

The Si_3N_4 ceramic and the reaction layer at the Si_3N_4 ceramic/filler alloy interface was considered to remain elastic, while plasticity was allowed in the 42CrMo steel and GM filler alloy. A von Mises yielding condition and isotropic hardening were assumed. The basic materials properties used in computations are given in Table 1. We introduced the following equations to calculate the mechanical properties for the composite. The elastic modulus (E) and thermal expansion coefficient (C) for the monolayer composite filler in GM filler alloy were expressed as follows [21]:

$$E_c = \frac{E_M[E_m V_r + E_r(V_r+1)]}{E_r V_m + E_m(V_r+1)} \quad (1)$$

$$C_c = \frac{C_m V_m K_m + C_r V_r K_r}{V_m K_m + V_r K_r} \quad (2)$$

where E is the elastic modulus and the subscripts c, m and r refer to the composite, matrix and reinforcement, respectively; V is the volume fraction of the reinforcement; K is the bulk modulus which can be calculated by the following equation: $K = E/(3\times(1-2\times\upsilon))$, where E and υ are elastic modulus and poisson's ratio, respectively.

The yield strength for the composite can be defined as follows [22]:

$$\sigma_{yc} = \sigma_{ym}(1+f_1)(1+f_d) \quad (3)$$

where σ_{yc} is the yield strength of the composite; σ_{ym} is the yield strength of the matrix; f_1 and f_d can be obtained by following:

$$f_1 = 0.5V_p \quad (4)$$

$$f_d = kG_m b\frac{\sqrt{r}}{\sigma_{ym}} \quad (5)$$

$$r = \frac{12\Delta\alpha\Delta T V_p}{bd_p(1-V_p)} \quad (6)$$

where V_p is the volume fraction of the reinforcement; G_m is the shear modulus of the matrix; b is the Burgers vector of the matrix; k is a constant, approximately 1.25; d_p is the particle size; $\Delta\alpha$ is the CTE difference between the matrix and reinforcement; ΔT is the difference between the processing and test temperatures.

3. Results and discussion

3.1. FEM results

To better focus on the nature of stress state in a brazed joint, the magnitude and distribution of the residual stresses were computed while the monolayer composite filler was inserted. Fig. 2 demonstrates the contour plots of computed axial (σ_{xx}), radial (σ_{yy}) and shear stresses (σ_{zz}) in a brazed joint, by inserted with Ag–Cu–Ti filler alloy incorporated with 10 vol% Mo particles. The residual stresses were constrained around the substrates/filler alloy interfaces. Even along the interface, its distribution was also not homogeneous. For σ_{xx}, the largest residual stress occurred at the edge of the substrates (Si_3N_4 ceramic and 42CrMo steel), and diminished away from the interface. The same trend was also observed for σ_{yy} and σ_{zz}, as shown in Figs. 2(b and c). We should emphasize the importance of the axial tensile stresses since it plays a key role in determining the joint bonding strength. Note that most ceramic can bear compressive stresses, but show

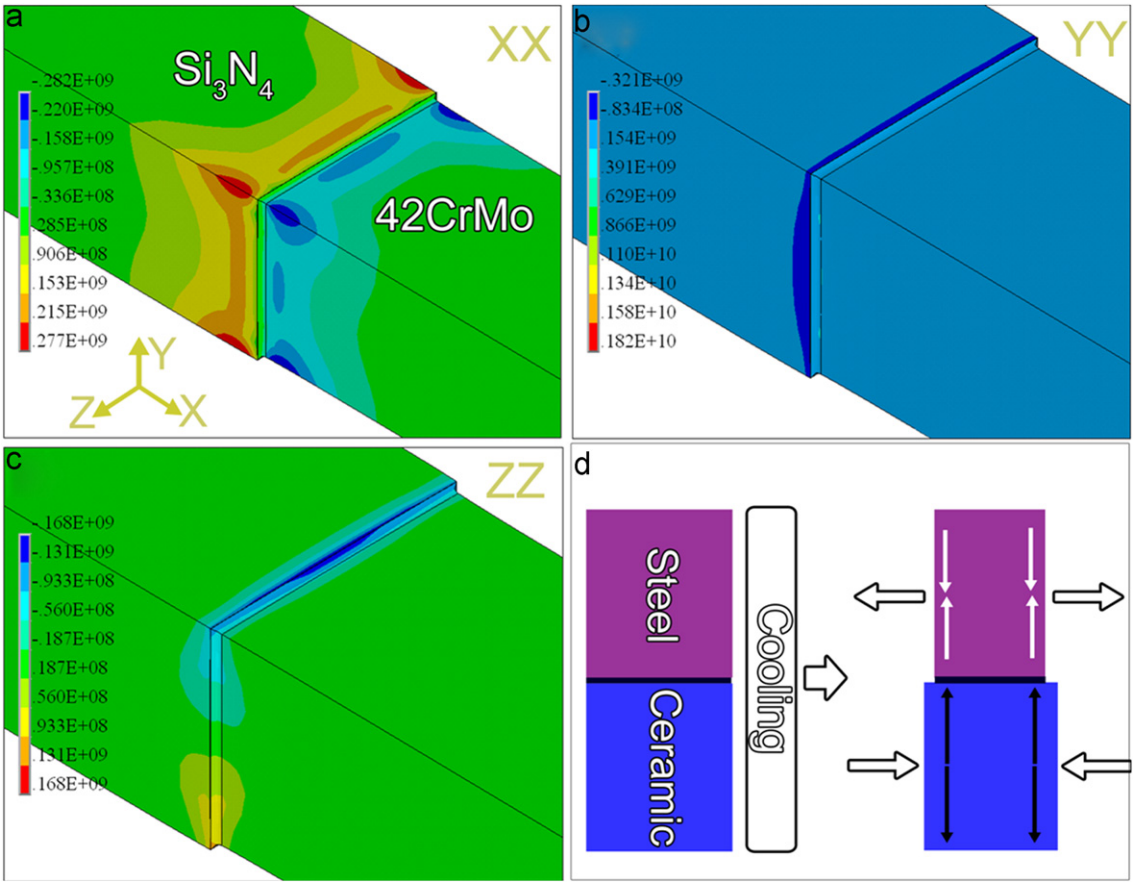

Fig. 2. Contours plots of the computed residual stress in the joint by inserting with Ag–Cu–Ti incorporated with 10 vol% Mo particles: (a) σ_{xx}; (b) σ_{yy}; (c) σ_{zz} and (d) schematic drawing showing the formation of the axial residual stresses.

poor ability in enduring the tensile stresses. As straightforwardly observed in Fig. 2(a), the maximal tensile stress could reach 277 MPa at the edge of Si_3N_4 ceramic, while the maximal compressive stress was found in the 42CrMo steel near the interface. The reasons for this are related to the fact that both the substrates should contract as they cooled from the brazing temperature. That say the 42CrMo steel should shrink more than the Si_3N_4 ceramic under the same temperature gradient since the CTE value for 42CrMo steel is far higher than that of Si_3N_4 ceramic. They could restrict deformation of the counterpart by the metallic brazing layer. Thus, at room temperature, the lower expansion material experiences a compressive stress on the whole, while the larger expansion material is in tension, as schematically demonstrated in Fig. 2(d). In order to balance those internal stresses, the axial tensile stresses should occur at the edge of Si_3N_4 ceramic, while the compressive stresses were present in the 42CrMo steel.

The residual stresses around the periphery of the whole joint are still an overriding concern by most researches, little attention was paid to the stress state inside the joint. We observed the distribution of axial stresses along different sections in the joint, as shown in Fig. 3. It is important to note that the stress distribution behaved in a diverse trend inside the joint. The distribution of the residual stresses was revealed in the section which was cut in the midline of the joint, as indicated in Fig. 3(b). The compressive stresses were observed in the Si_3N_4 ceramic, while the tensile stresses were present in the 42CrMo steel. In addition to this, no stress singularity was observed in the section. Fig. 3(c) demonstrates the stresses distribution in the filler alloy at the right side of the interfacial reaction layer. A large decrease in the stress magnitude and uniform stress distribution were found, which means the residual stresses exhibited a large variation in a small range in the brazed joint. Fig. 3(d) shows the stress distribution in the brazing layer, no stress singularity was also observed and the maximal stress value was dramatically dropped.

Fig. 4 indicates the contour plots of equivalent plastic strain ε^p in the joint. A plot of the plastic strain variation along one of the edges clearly indicates that the plasticity was entirely confined within the filler metal layer. The contact position between the interfacial reaction layer and filler alloy was defined as the reference point. As demonstrated in Fig. 4, the largest plastic strain was constrained in the filler alloy near the interfacial reaction layer at the Si_3N_4 ceramic/filler alloy interface, and decreased close to the 42CrMo steel. Actually, it does not mean that the plastic strain always occurs in a brazed joint. We cannot observe them if the maximal residual stress in the joint does not exceed the yield stress of the filler alloy. With the aid of Eq. (3), the yield stress in the monolayer

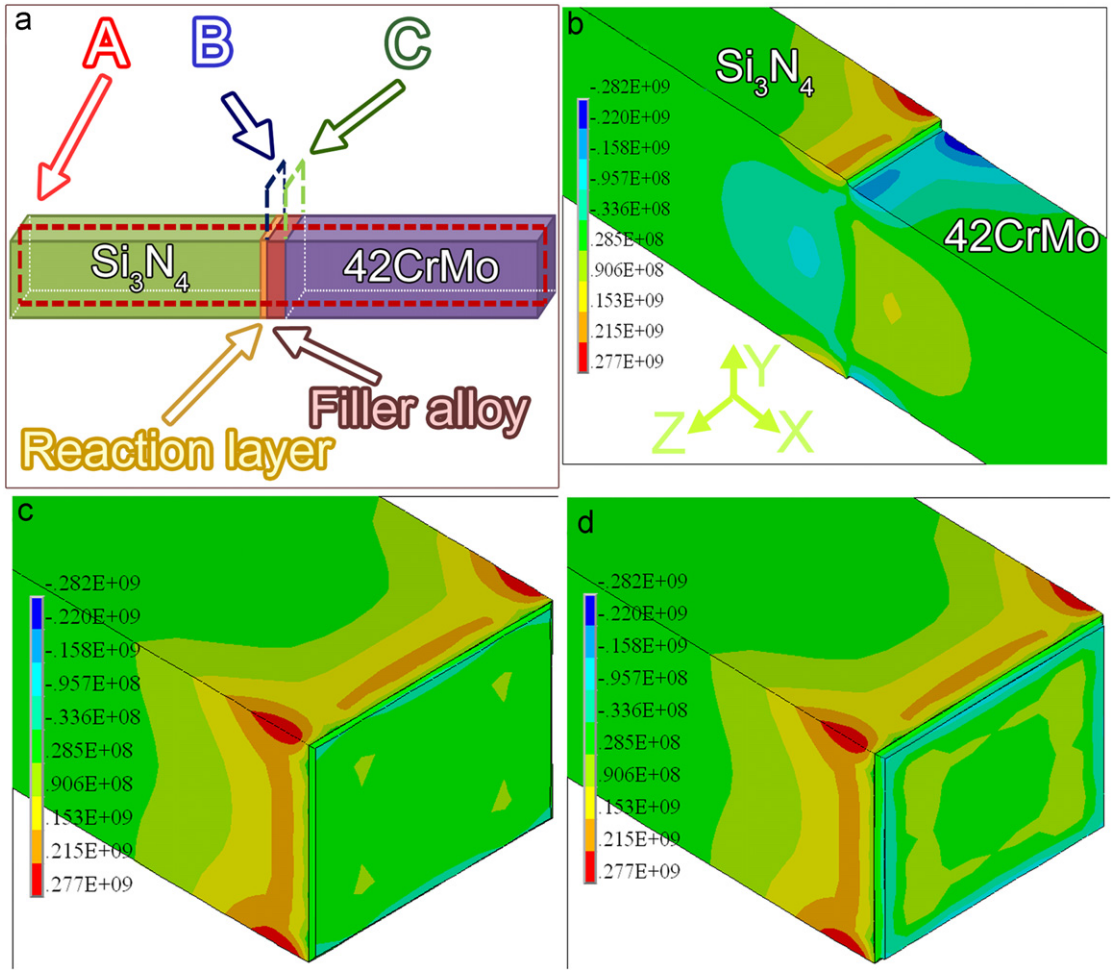

Fig. 3. Distribution of axial residual stresses along different sections in the joint: (a) the schematic drawing showing the positions of different sections; the distribution of axial stresses in the section (b) A: in the midline of the joint; (c) B: at the right of the interfacial reaction layer at the Si_3N_4/filler alloy interface; (d) C: at the right of the filler alloy near the 42CrMo steel.

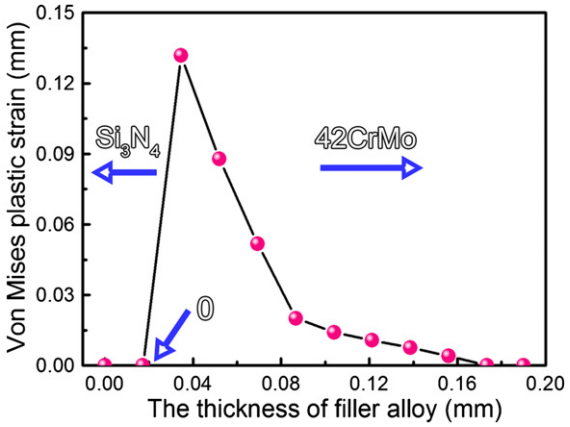

Fig. 4. Contours of equivalent plastic strain ε^p along the edge relative to the origin which was constrained in three directions.

composite filler with 10 vol% Mo particles addition was 254.6 MPa, which is lower than the maximal residual stress of 277 MPa. So, its occurrence in the joint was reasonable. Furthermore, we should keep in mind that the Si_3N_4 ceramic and 42CrMo steel were joined by the filler alloy. Compared to 42CrMo steel, however, the Si_3N_4 ceramic should contract less owing to its low CTE on cooling from the brazing temperature. To produce joining, the larger plastic strain should occur in the brazing layer near the Si_3N_4 ceramic. Also, and most importantly, it should be noted that the large strain in the filler alloy was not detrimental to the joint strength due to its favorable ability of deformation.

In order to create a smooth CTE change along the joint, a model based on two layers GM filler alloy was adopted and the residual stresses in the joint were computed. Typically, the layer with a high content of Mo particle addition (20–40 vol%) was set close to Si_3N_4 ceramic, while the layer with lower content of Mo particles addition (5–10 vol%) was put near the 42CrMo steel. When the layer with the content of 5 vol% Mo particles was set near the 42CrMo steel, the layer with the content of 20 vol%–40 vol% Mo particles was set close to the Si_3N_4 ceramic. After that, the layer with content of 10 vol% Mo particles was put near the 42CrMo steel, then varied the content of Mo particles in another layer adjacent to Si_3N_4 ceramic, also from 20 vol% to 40 vol%. Fig. 5(a) shows the

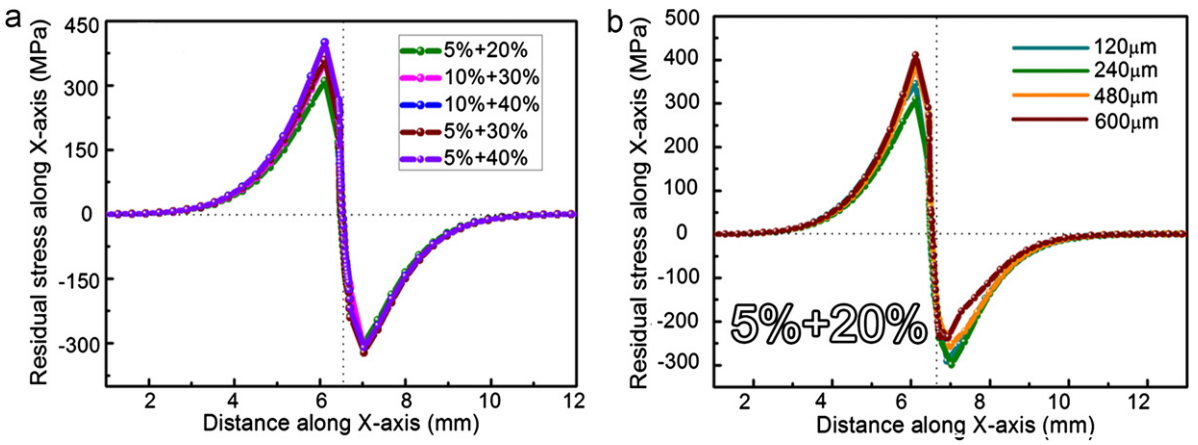

Fig. 5. (a) Computed axial stresses for the two layers GM specimens along one of the edges of the joined materials; (b) GM thickness on the effect of the residual stresses in the joint by inserting with 5 vol% Mo+20 vol% Mo GM.

computed axial stresses for the two layers GM specimens along one of the edges in the brazed joint. Similar to the stress profiles described previously, the peak tensile stresses were always observed in the Si_3N_4 ceramic while the compressive stress was present in the 42CrMo steel. A key phenomenon should be demonstrated here, the residual stresses in the joint were increasing if the higher content of Mo particles was incorporated. The tensile residual stress was only 314 MPa while 5 vol% Mo+20 vol% Mo GM filler alloy was used, whereas, it was increased by approximately 30% while the 10 vol% Mo+40 vol% Mo was introduced. Our results are entirely at odds with the prevalent notion that the gradient filler alloy could cause a smooth CTE mismatch and help to relieve the residual stresses. Fig. 5(b) shows the thickness of GM filler alloy on effect of the residual stresses in a brazed joint. The composition of GM used was 5 vol% Mo+20 vol% Mo and its thicknesses were 120 μm, 240 μm, 480 μm and 600 μm, respectively. One may observe that the residual stress in the Si_3N_4 ceramic could reduce to a minimum while the GM thickness was 240 μm. The brazing layer can aid in relaxing the residual stress by its creep and yield mechanisms. However, it does not mean that the thicker the brazing layer is, the higher the joint strength will be. Computation data so far inspire us that an optimum thickness should be selected during brazing. The results reported here could guide us to choose the thickness of GM filler alloy in the subsequent experiment.

We also examined the effect of multilayer GM structure in mitigating the residual stresses, as displayed in Fig. 6. One layer, double layers, three layers, four layers, six layers were compared in the figure. The total thickness of the GM was 240 μm, and assumed that the thickness of each layer in the GM filler alloy was equal. There is no doubt that the identical stress distribution modes were observed. The peak compressive stresses in the 42CrMo steel varied less with increasing layer numbers in the GM. The tensile stresses in the Si_3N_4 ceramic, however, showed a different trend. We were surprised to observe that the minimal stress was obtained while monolayer composite filler was

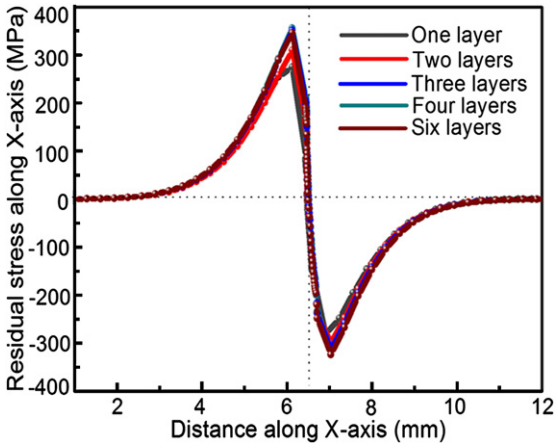

Fig. 6. Computed axial stresses for the multilayer GM structure along one of the edges of the joined materials. (The compositions for the GM structure are as follows. One layer: 10 vol% Mo; two layers: 5+20; three layers: 5+15+30; four layers: 5+10+20+30; six layers: 5+10+15+20+25+30).

inserted. The result contradicted the viewpoints of lots of researchers [16,17,19,20,23,24], who believed that the more layers in the GM could reduce the residual stress due to its smooth change in CTE and elastic modulus. We should note that the multilayer GM structure can actually produce a successive change in the CTE and elastic modulus along the joint, aiding in improving the joint strength. However, for the sake of forming a continuous GM filler alloy, the brazing layer with a high content of Mo particles addition should be inevitably inserted. The above operation can greatly impair the plasticity of the filler alloy. We have reported that the joint strength was deteriorated when the content of Mo particles exceeded 10 vol% in the monolayer composite filler [15]. The lower strength was caused by the poor plasticity and pores in the brazing layer. Even the filler metal layer with a high content of reinforcement incorporation can decrease the CTE mismatch to a large extent. The increase of yield stress in the filler alloy can counteract its influences. In other words, the

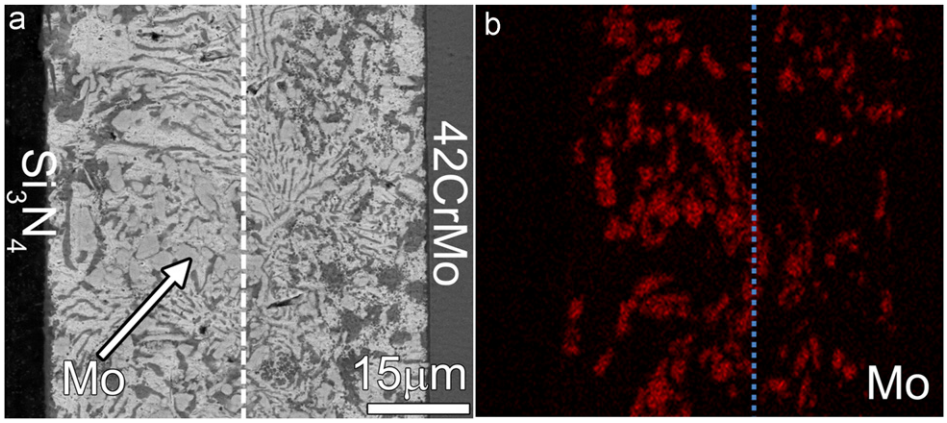

Fig. 7. Microstructure and Mo element distribution images in the joint brazed by using 5 vol% Mo+20 vol% Mo GM filler alloy.

ability of plastic deformation in the filler alloy was one of the governing factors that determined the joint strength.

3.2. Experimental analysis

Fig. 7 shows the microstructure of the joint brazed with a two layers GM filler alloy, namely 5 vol% Mo+20 vol% Mo. A sound reaction layer was formed at each substrate/filler alloy interface. At the Si_3N_4 ceramic/filler alloy interface, the reaction layer was composed of TiN and Ti_5Si_3, with the TiN close to the Si_3N_4 ceramic. A double reaction layer consisting of Fe_2Ti and FeTi was also formed adjacent to 42CrMo steel, with Fe_2Ti near the steel. The central part of the joint was composed of Ag based solid solution, Cu based solid solution, Mo particles together with few Cu–Ti intermetallics. As demonstrated in Fig. 7(b), Mo particles were uniformly dispersed in each layer, achieving the original intention for which the structure we designed.

Fig. 8 displays SEM micrographs of the Si_3N_4 ceramic/42CrMo joints brazed with different GM structure. The Mo particles spread randomly in each layer, which was essential in achieving a smooth CTE and elastic modulus change along the joint. In addition, the thickness of reaction layer at the Si_3N_4 ceramic/filler alloy interface was increasing by elevating the layer numbers. Its thickness was less than 2 μm when the monolayer was used, whereas, it increased to 3.5 μm while three layers were introduced. One may speculate that more layers could increase the total thickness of the filler alloy, increasing the total Ti amount and thus providing sufficient Ti element to react with Si_3N_4 ceramic.

Fig. 9(a) demonstrates the three-point bending test results of the brazed Si_3N_4/42CrMo joints. The maximal bending strength could reach 587.3 MPa by using monolayer composite filler with 10 vol% Mo particles addition, which was 414.3% higher than the average strength for the case without Mo addition. The residual stresses that resided in the joint were probably responsible for the variation of the joint strength. As shown in the picture, the experimental results correlated well with the finite element predictions. Three types of failure mode were observed after bending tests, as presented in Figs. 9(b–e). The first type is shown in Fig. 9(b), in which fracture initiated at the edge of Si_3N_4 ceramic near the interface where the greatest tensile residual stresses concentrated, and then propagated in the ceramic, forming a bowed fracture pattern. This kind of fracture type indicates a considerable thermal residual stress was resided in the joint. Another type (Fig. 9c), for the case of the joint brazed with the monolayer composite filler with 10 vol% Mo addition, fracture altered between the Si_3N_4 ceramic and filler alloy. The fracture mode with no evidence of significant residual stresses implied that the crack initiated in the ceramic near the interface, and extended into the filler alloy under external load. Fig. 9(d) shows the third type, in which fracture occurs in the brazing layer, corresponding to the joint brazed with two or three layers GM. The fracture mode indicates a lower joint strength, and the following two factors were contributed to it. On the one hand, more layers in the GM could induce a higher residual stresses in the joint, as demonstrated in Fig. 9(a). On the other hand, in order to form a continuous GM filler alloy, the brazing layer with the higher content of Mo particles should be inevitably introduced. Therefore, partial Mo particles could not be wetted due to the insufficient amount of liquid filler during brazing. Lots of pores were thus observed on the fracture surface, as demonstrated in Fig. 9(e).

4. Discussions

For ceramic joining, many factors are involved in obtaining a robust joint, i.e. chemical reaction between materials during joining, thermal expansion mismatch between components, processing variables, geometry of the components etc. The challenges can be classified into chemical or mechanical factor in nature [25]. Significant advances have been made in the field of chemical control. The active element, i.e. Ti, Zr, Hf, can be incorporated in the filler alloy. In the study, the Ti-activated filler alloy was used and a sound reaction layer was formed at each substrate/filler alloy interface after brazing. A remarkable phenomenon should be clarified here, by observing the fracture surface after bending, no cracking in the reaction

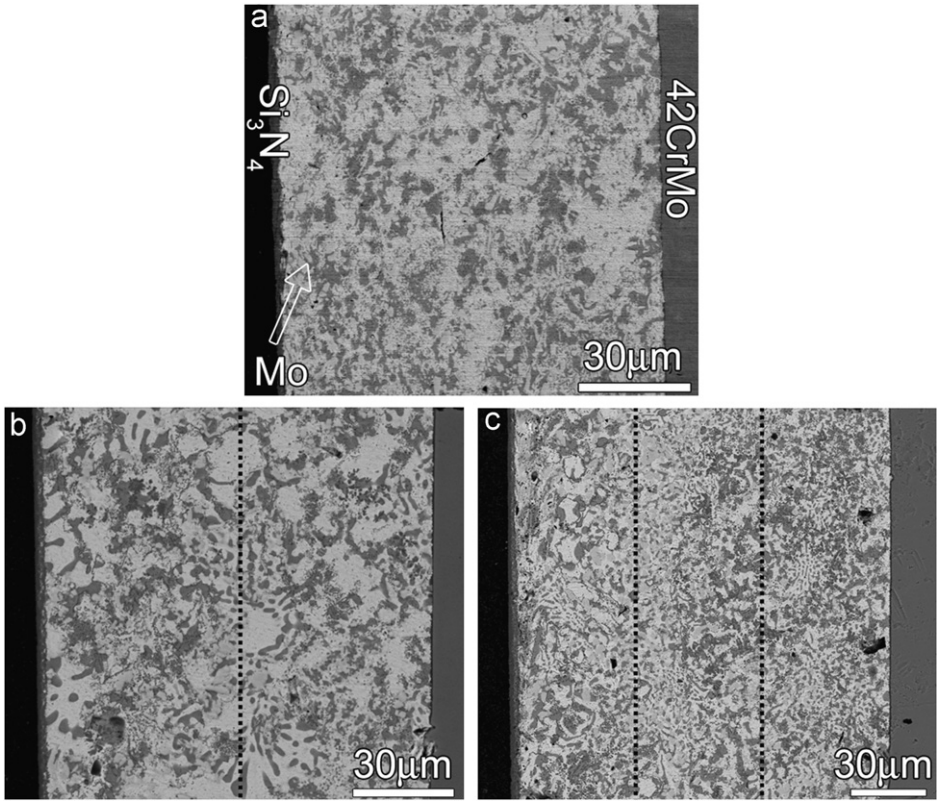

Fig. 8. SEM micrographs for the joints brazed with different GM structure: (a) one layer: 10 vol% Mo; (b) two layers: 5+20 vol% Mo; (c) three layers: 5+15+30 vol% Mo.

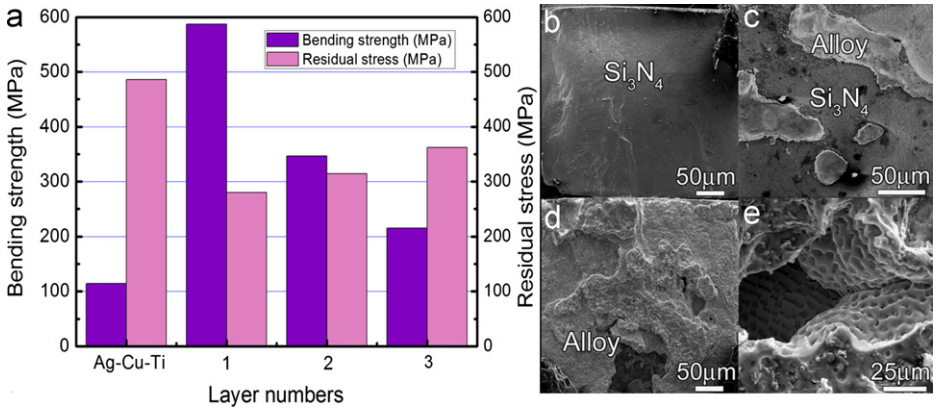

Fig. 9. Bending strength versus different GM structure (a) and fractography for the joints brazed with: (b) Ag–Cu–Ti, (c) one layer, (d) two or three layers and (e) the magnified photograph in (d).

layer was found, which means the interfacial bonding was strong enough in the research. Thus, for a well-bonded joint, the thermal expansion mismatches between the joined components and the resulting residual stresses was the critical factor to determine the joint strength. The residual stress, which was always concentrated at the edge of the substrates near the interface, is the dynamic force for the crack initiation and subsequent propagation in the ceramic joints under external loads. Some kinds of interlayers were usually introduced into compensating for the residual stress, i.e. soft metal interlayers, hard metal interlayers. A soft metal interlayer, such as Cu or Ni, reduces the residual stress by its elastic, plastic, and creep deformation. The hard metal interlayer, whereas, aids stress accommodation by decreasing CTE mismatch between the joining materials. We should note that the residual stresses resided in the joint were directly caused by CTE mismatch between the joined materials, yet the plastic deformation in the filler alloy could relax partial stresses while the maximal residual stresses exceeds the yielding point of the filler alloy. From above discussion, one can infer that the residual stresses level in the joint was

essentially controlled by the CTE mismatch and the ability of plastic deformation in the filler alloy. A key question should be addressed: how could they cooperate to obtain the joint with the minimal residual stresses level? In the research, the FEM analysis in conjunction with experiments provided a hint to answer the above question. Actually, by increasing layer numbers in the GM filler alloy, two effects were induced: on the one hand, more layers in the filler alloy could form a smooth gradual composition transition, which will reduce the CTE mismatch and accordingly induce the lower residual stresses; on the other hand, the layer with higher content of Mo particles addition should be inevitably introduced in the multilayer GM, which will sacrifice the ability of the filler alloy to mitigate the residual stresses through its plastic deformation. In order to obtain a robust joint, a trade-off should be accomplished between the two factors to minimize the residual stresses. In the research, the robust joint was obtained while the monolayer with 10 vol% Mo addition was adopted. Only the monolayer by incorporating 10 vol% Mo particles was enough to obtain the highest joint strength, that said the lowering of CTE mismatch in combination with the allowable plastic deformation in the filler alloy was contributing the joint strength, note that the CTE was reduced merely 71% in the situation. For the joint brazed with multilayer GM filler alloy, even a smooth CTE change across the joint could result in the lower residual stresses, the total residual stress level was always higher than that present in the joint brazed with the monolayer owing to their poor plasticity. So, we can conclude the ability of plastic deformation in the filler alloy was essential in mitigating the residual stresses and determining the stress level in the joint.

How could we quantify the factors that determine the residual stresses level in the joint? For fully elastic conditions, the thermal stress is determined by following well-known equation [26]

$$\sigma = \frac{E_M E_C}{E_M + E_C}(T_{free} - T_{room})(\sigma_M - \sigma_C) \quad (7)$$

where E is Young's modulus and σ is the linear thermal expansion coefficient; T_{free} is the free-stress temperature, which was believed to be 780 °C for Ag–Cu–Ti; the subscript M and C represent metal and ceramic, respectively. For Ag–Cu–Ti, the calculated residual stresses in the Si_3N_4 ceramic could reach 743.6 MPa by above equation, close to the fracture strength of Si_3N_4 ceramic (800 MPa). Actually, an average bending strength of 114.2 MPa was obtained, which means the above equation neglecting the plasticity in the filler alloy was not applicable. In addition, we have employed Digital Image Correlation method to characterize the local deformation in the filler alloy, and 1.55% ε_{xx} could be observed after bending test, an indication of high plastic deformation in the filler alloy. Actually, most of the filler alloy that we choose to join the ceramic could deform plastically and the deformation was considered a significant way to accommodate the residual stresses. The effect of plastic deformation on the magnitude of residual stresses is not fully understood yet, and no metric was built to estimate the stress while considering the plastic deformation in the filler alloy. The FEM method was approved to provide useful information in estimating the residual stress level in the joint while considering both the CTE mismatches and plastic deformation in the filler alloy.

5. Conclusions

The residual stresses were studied experimentally by using GM filler alloy in a model Si_3N_4 ceramic–42CrMo steel joint. An elastic–plastic FEM model was used to investigate the residual strains and stresses in the joint, and to study the role of the GM compositions, layer numbers and thicknesses on the predicted stresses. The following conclusions were drawn.

(1) During the Si_3N_4 ceramic–42CrMo steel joining, the peak tensile axial stresses were always found at the edge of Si_3N_4 ceramic near the interface, while the peak compressive stresses occurred in the 42CrMo steel. In addition, the largest plastic strain was concentrated in the filler alloy near the interfacial reaction layer at the Si_3N_4 ceramic/filler alloy interface, and its value decreased close to the 42CrMo steel.
(2) The thickness of the brazing layer had a far-reaching impact on the joint strength. For 5 vol% Mo + 20 vol% Mo GM filler alloy, the optimum thickness was 240 μm, which produced the minimum residual stresses in the joint.
(3) The FEM results indicated that the joint brazed with monolayer incorporated with 10 vol% Mo particles produced the lowest residual stresses, which was also validated by experiments. The multilayer GM structure with a more smooth CTE change across the joint was believed to lead to a high quality joint theoretically, yet they failed owing to their poor plasticity.
(4) The FEM results coupled with experiments indicated that the CTE mismatch between the joined materials and the ability of plastic deformation in the filler alloy was two factors that determine the residual stresses level in the joint. More importantly, the ability of plastic deformation in the filler alloy was one of the key factors to influence the residual stresses level in the joint, which should be drawn strong attention in designing the filler alloy.

Acknowledgments

This work was financially supported by the National Nature Science Foundation of China under Grant nos. 50975064, 51021002and 50902029. We also thank Harbin Special Funds for Technological Innovation Research Projects under the number of 2010RFQXG022.

References

[1] M. Vila, C. Prietow, P. Miranzo, M.I. Osendi, J.M. Del Rı′o, J.L. Pe′rez-Castellanos, Measurements and finite-element simulations of residual stresses developed in Si_3N_4/Ni diffusion bonds, Journal of the American Ceramic Society 88 (9) (2005) 2515–2520.

[2] Y. Zhou, F.H. Bao, J.L. Ren, T.H. North, Interlayer selection and thermal stresses in brazed Si_3N_4-steel joints, Materials Science and Technology 7 (1997) 863–868.

[3] X. Wang, L.F. Cheng, S.W. Fan, L.T. Zhang, Microstructure and mechanical properties of the GH783/2.5D C/SiC joints brazed with Cu–Ti+Mo composite filler, Materials and Design 36 (2012) 499–504.

[4] T.S. Lin, M.X. Yang, P. He, C. Huang, F. Pan, Y.D. Huang, Effect of in situ synthesized TiB whisker on microstructure and mechanical properties of carbon–carbon composite and TiBw/Ti–6Al–4V composite joint, Materials and Design 32 (2011) 4553–4558.

[5] S.P. Kovalev, P. Miranzo, M.I. Osendi, Finite element simulation of thermal residual stresses in joining ceramics with thin metal interlayers, Journal of the American Ceramic Society 81 (9) (1998) 2342–2348.

[6] Soon-Bok Lee, Jong-Ho Kim, Finite-element analysis and X-ray measurement of the residual stresses of ceramic/metal joints, Journal of Materials Processing Technology 67 (1997) 167–172.

[7] Y.M. He, J. Zhang, C.F. Liu, Y. Sun, Microstructure and mechanical properties of Si_3N_4/Si_3N_4 joint brazed with Ag–Cu–Ti+SiCp composite filler, Materials Science and Engineering A 527 (2010) 2819–2825.

[8] K. Suganuma, Y. Miyamoto, M. Koizumi, Joining of ceramics and metals, Annual Review of Materials Science 18 (1998) 47–73.

[9] Y. Zhou, K.J. Lkeuchi, T.H. North, Z.R. Wang, Effect of plastic deformation on residual stresses in ceramic/metal interfaces, Metallurgical Transactions A 22A (1991) 2822–2824.

[10] Jin-Woo Park, A Framework for Designing Interlayers for Ceramic-to-Metal Joints, Ph.D. Thesis, Massachusetts Institute of Technology, Boston, Massachusetts, 2002.

[11] M.G. Zhu, D.D.L. Chung, Active brazing alloy containing carbon fibers for metal–ceramic joining, Journal of the American Ceramic Society 77 (10) (1994) 2712–2720.

[12] M.G. Zhu, D.D.L. Chung, Improving the strength of brazed joints to alumina by adding carbon fibers, Journal of Materials Science 32 (1997) 5321–5333.

[13] G. Blugan, J. Janczak-Rusch, J. Kuebler, Properties and fractography of Si_3N_4/TiN ceramic joined to steel with active single layer and double layer braze filler alloys, Acta Materialia 52 (2004) 4579–4588.

[14] G. Blugan, J. Kuebler, V. Bissig, J.J. Rusch, Brazing of silicon nitride ceramic composite to steel using SiC-particle-reinforced active brazing alloy, Ceramics International 33 (2007) 1033–1039.

[15] Y.M. He, J. Zhang, Y. Sun, C.F. Liu, Microstructure and mechanical properties of the Si_3N_4/42CrMo steel joints brazed with Ag–Cu–Ti+Mo composite filler, Journal of the European Ceramic Society 30 (2010) 3245–3251.

[16] B.H. Rabin, R.L. Williamson, H.A. Bruck, X.L. Wang, T.R. Watkins, Y.Z. Feng, D.R. Clarke, Residual strains in an Al_2O_3–Ni joint bonded with a composite interlayer: experimental measurements and FEM analyses, Journal of the American Ceramic Society 81 (6) (1998) 1541–1549.

[17] C.S. Lee, X.F. Zhang, G. Thomas, Novel joining of dissimilar ceramics in the Si_3N_4–Al_2O_3 system using polytypoid functional gradients, Acta Materialia 49 (2001) 3775–3780.

[18] X.R. Zeng, J.N. Tang, P. Xiao, Fabrication and thermal properties of a YSZ–NiCr joint with an interlayer of YSZ–NiCr functionally graded material, Journal of the European Ceramic Society 23 (2003) 1847–1853.

[19] R.L. Williamson, B.H. Rabin, J.T. Drake, Finite element analysis of thermal residual stresses at graded ceramicmetal interfaces. Part 1. Model description and geometrical effects, Journal of Applied Physics 74 (2) (1993) 1310–1320.

[20] J.T. Drake, R.L. Williamson, B.H. Rabin, Finite element analysis of thermal residual stresses at graded ceramic-metal interfaces. Part II. Interface optimization for residual stress reduction, Journal of Applied Physics 74 (2) (1993) 1321–1326.

[21] I.A. Ibrahim, F.A. Mohamed, E.J. Lavernia, Particulate reinforced metal matrix composites-a review, Journal of Materials Science 26 (1991) 1137–1156.

[22] Z. Zhang, D.L. Chen, Consideration of Orowan strengthening effect in particulate-reinforced metal matrix nano-composites: a model for predicting their yield strength, Scripta Materialia 54 (2006) 1321–1326.

[23] C.S. Lee, L.C.D.E. Jonghe, G. Thomas, Mechanical properties of polytypoidally joined Si_3N_4–Al_2O_3, Acta Materialia 49 (2001) 3767–3773.

[24] K. Pietrzak, D. Kalíński, M. Chmielewski, Interlayer of Al_2O_3–Cr functionally graded material for reduction of thermal stresses in alumina-heat-resisting steel joints, Journal of the European Ceramic Society 27 (2007) 1281–1286.

[25] Lea Wiese Jocelyn, Strength of Metal-to-Ceramic Brazed Joints, MD Thesis, Massachusetts Institute of Technology, Boston, Massachusetts, 2000.

[26] D. Peteves Stathis, G. Nicholas Michael, Evaluation of brazed silicon nitride joints: microstructure and mechanical properties, Journal of the American Ceramic Society 79 (6) (1996) 1553–1562.